A potential field approach to the modeling of route choice in pedestrian evacuation

Ren-Yong Guo[1], Hai-Jun Huang[2] and S.C. Wong[3]

[1] College of Computer Science, Inner Mongolia University, Hohhot 010021, People's Republic of China

[2] School of Economics and Management, Beijing University of Aeronautics and Astronautics, Beijing 100191, People's Republic of China

[3] Department of Civil Engineering, The University of Hong Kong, Pokfulam Road, Hong Kong, People's Republic of China

E-mail: buaa_guorenyong@126.com, haijunhuang@buaa.edu.cn and hhecwsc@hku.hk

Abstract. This study proposes a potential field algorithm for formulating pedestrian route choice behavior during evacuation in individual-based models with discrete space representation. The potential field reflects the effect of the route distance, pedestrian congestion and route capacity on route choice. Numerical simulations show that the developed model can reproduce more route choice modes in a scenario compared with several existing models. Three groups of pedestrian evacuation experiments are conducted and the proposed model reproduces pedestrian route choices effectively.

Key words: cellular automata, stochastic particle dynamics (theory), traffic and crowd dynamics, traffic models

1. Introduction

Increases in city and urban populations and mass events have raised interest among researchers and authorities in problems of pedestrian-dynamics [1]-[4]. Pedestrian behavior in different scenarios has been investigated using mathematical models and computer simulations [5, 6]. These models and simulations help to shed light on pedestrian-dynamics problems and influence engineering decisions that maintain public facility service levels and ensure pedestrian safety.

When pedestrians evacuate a closed area such as a meeting room, supermarket or theater or an open area such as a plaza or park, their choice of route is a critical behavioral reaction that affects the efficiency of their evacuation. Once they cannot appropriately select an evacuation route, a phenomenon in which many individuals collect on a few routes is likely to occur, leading to inefficient evacuation or even accidents caused by jamming. A study of pedestrian route choice behavior would lay the groundwork for route planning and finding meaningful locations for signs in pedestrian facilities. In this paper, we focus on the subject of pedestrian route choice, which depends on the prerequisite that they are familiar with the layout of the area and dynamic distribution of all individuals during evacuation so that the quickest evacuation can be implemented in principle.

Route choice can be modeled using network-based models [7]-[12]. In this class of models, the spatial layout of a facility is represented by a network based on the facility's actual structure. Accordingly, each node in the network represents a section of the pedestrian space in the facility irrespective of its physical dimensions. These nodes are connected by arcs that represent the actual openings between separate components. This class of models is generally used to form solutions to optimization problems and involves link disutility or cost functions. In these optimization problems, the numbers of pedestrians in these nodes are seen as decision variables. However,

several issues must be considered carefully before applying this class of models to route choice. First, it does not consider the fact that when the number of pedestrians in each section of the pedestrian space is fixed, their distribution in each section affects their choice of evacuation route. Second, while the number of pedestrians assigned to each route is known in the optimization problems, how the pedestrians are distributed in the route is unclear. Third, the link walking time functions are difficult to determine.

To avoid the aforementioned issues, route choice can be modeled in individual-based models using either continuous space representation [13]-[15] or discrete lattice space [16]-[26]. In the individual-based models, each pedestrian is considered as a discrete individual, and the position update of each individual is formulated by a continuous or discrete dynamical system. The individual-based models mainly include the social force [5], lattice gas [27], cellular automata [1] and discrete choice models [3].

In individual-based models with discrete lattice space, pedestrian route choices are formulated using the potential field of the lattice, i.e., the floor field in [1] and [28]. The potential is generally used to measure the route distance from the lattice site to the destination, the congestion of pedestrians en route to the destination or the capacity of routes to the destination; this allows these factors to be taken into account in a unified and simple way. Varas et al. [16] and Huang and Guo [17] proposed a category of algorithms to compute the potential of each lattice site that considers only the route distance, thereby formulating pedestrian route choices to multiple exits.

Kretz [18] and Hartmann [21] considered the effects of not only route distance but also pedestrian congestion on route choice using the potential of space. For some scenarios, a location’s congestion affects the route choices of not only nearby

individuals but also pedestrians who are far from the location; however, for other some scenarios, a location's congestion affects only the route choices of nearby individuals and has no effect on the route choices of pedestrians who are far from the location. Guo and Huang [19] and Alizadeh [23] formulated pedestrian route choices in buildings with multiple exits and obstacles using a class of potentials that weigh route distance and pedestrian congestion. Guo and Huang [19] used the number of pedestrians selecting each exit to reflect the effect on an individual, and Alizadeh [23] used the number of pedestrians on frontal routes to exits.

Zhao and Gao [22] and Xu and Huang [25] formulated pedestrian route choice non-uniformly distributed in a facility while considering route distance and capacity. Zhao and Gao [22] used the free spaces near each exit to reflect the effect of capacity on each individual's route choice, and Xu and Huang [25] used the free spaces near both each exit and each individual. However, neither study acknowledged that the free spaces between the two regions also affect route choice. In addition, their models probably become unreliable when there are obstacles in the facility.

Guo and Huang [20] developed a method for computing the potential of discrete space that measures route distance, pedestrian congestion and route capacity. Capacity is reflected in the width of each link. However, when the widths of all links in a facility are equal, their model cannot be used to formulate the effect of capacity on the route choice. Zhang et al. [26] also established a potential field for pedestrian dynamics in individual-based models with discrete lattice space. The potential of each lattice site is defined as the minimal cost of traveling from the lattice site to the destination. The cost is related to the route distance and pedestrian density on front routes to the destination. However, the potential field cannot control the ratio of pedestrians selecting each route. In fact, real pedestrians are not completely rational

and sometimes select routes with non-minimal costs. Therefore, to formulate real pedestrian route choice behavior, a potential field should be capable of controlling the ratios of pedestrians selecting each route.

We propose a potential field algorithm to formulate the route choice behavior of evacuating pedestrians in individual-based models with discrete space representation. The potential field has the following three properties. First, it reflects the effect of route distance, pedestrian congestion and route capacity on the route choice. The effect of capacity on an individual's route choice is reflected in the free space in front of the individual. Second, it can formulate more route choice modes in a scenario than several existing potential fields. That is to say, by adjusting the parameters of the algorithm, the number of pedestrians selecting each route varies in a larger interval. Thus, the algorithm is more likely to be used to reproduce real pedestrian route choice behavior. Third, it can formulate the route choice of pedestrians evacuating a facility with internal obstacles and multiple exits.

In Section 2, we introduce the algorithm and an associated individual-based pedestrian model with discrete space representation. In Section 3, we use numerical simulation to show that the potential algorithm can reproduce phenomena that several existing potential field algorithms cannot reproduce. Further, we conduct three groups of pedestrian evacuation experiments in a classroom. These experiments and a comparison of experiment results and model simulations are described in Section 4. Section 5 concludes the paper.

2. Algorithm and Model Description

While the proposed model is applied to simulate pedestrian evacuation from a closed

area with internal obstacles and n exits, it can also be applied to simulate pedestrian route choices in open areas such as plazas and parks. Pedestrian space is represented by two-dimensional square lattices. Each lattice site can be either empty or occupied by an obstacle or exactly one pedestrian. In each discrete time step Δt, the positions of all pedestrians are updated in a random sequence.

In each time step Δt, each pedestrian moves only one lattice site in the horizontal or vertical directions (i.e., the Manhattan Metric) or remains unmoving. When at least one direction of movement is available, the pedestrian moves one lattice site in a horizontal or vertical direction. The choice of direction is governed by the transition probability, which represents the possibility that the pedestrian moves the distance of a lattice site in each direction. If we let the probability of transition from one lattice site (i, j) into a neighboring lattice site (i_0, j_0) in the horizontal or vertical directions be $P_{(i,j)\to(i_0,j_0)}$, it is computed as follows:

$$P_{(i,j)\to(i_0,j_0)} = U \exp(-\varepsilon p_{i_0 j_0})(1 - o_{i_0 j_0}), \quad (1)$$

where U is a normalization factor for ensuring that $\sum_{(i_0,j_0)} P_{(i,j)\to(i_0,j_0)} = 1$.

In equation (1), $p_{i_0 j_0}$ is the potential of the lattice site (i_0, j_0). The potential of a lattice site is used to reflect the total effect of the route distance from the lattice site to the exit, the pedestrian congestion on the frontal route to the exit and the capacity of the frontal route to the exit. The potential is directly proportional to the route distance and the degree of congestion and is inversely proportional to the size of the frontal free space. The potential influences the transition probabilities in such a way that a movement in the direction of a smaller potential is preferred.

In equation (1), ε (>0) is a sensitivity parameter for scaling the potential, and

parameter $o_{i_0 j_0}$ represents whether a neighboring lattice site (i_0, j_0) is occupied by a pedestrian, obstacle or wall. It is 1 if the lattice site is occupied and 0 otherwise. When all four neighboring lattice sites in the horizontal and vertical directions (i.e., the von Neumann neighborhood) are occupied, the pedestrian in this lattice site remains unmoving.

The n exits are numbered from 1 to n. Let e_{ij} be the exit serial number of lattice site (i, j), which indicates that the potential of lattice site (i, j) is iteratively computed by the potential of the lattice sites occupied by exit e_{ij}. The algorithm for computing the potential of lattices in the area is summarized by the following steps (Note that parameters d_k, δ, λ, α and β involved in this algorithm are specified later).

Step 1. For each lattice site (i, j) occupied by a wall or obstacle, its potential $p_{ij} = +\infty$.

Step 2. For each lattice site (i, j) occupied by exit k $(=1,2,\cdots,n)$, its potential $p_{ij} = 0$, and set $e_{ij} = k$.

Step 3. For each k $(=1,2,\cdots,n)$, set d_k as the number of lattice sites occupied by exit k.

Step 4. For each lattice site (i, j) with a neighboring lattice site (i_0, j_0) occupied by an exit in the horizontal or vertical directions, set its potential $p_{ij} = 1$, set $e_{ij} = e_{i_0 j_0}$, and it is added into the set of lattices that need to be checked.

Step 5. For each k $(=1,2,\cdots,n)$, set $d_k \leftarrow d_k + \bar{m}_k$, where $\bar{m}_k$ is the number of lattice sites, which are in the set of lattices that need to be checked, satisfy $e_{ij} = k$ and are not occupied by pedestrians.

Step 6. Set $\delta \leftarrow 1$.

Step 7. For each lattice site (i, j) in the set of lattices that need to be checked, if $\delta \le p_{ij} < \delta + 1$, then check its neighboring lattice sites (i_0, j_0) in all eight directions

(i.e., the Chessboard Metric) and remove the lattice site (i, j) from the set of lattices that need to be checked. If the potential $p_{i_0 j_0}$ of the lattice site (i_0, j_0) has not been determined, then set a temporary exit serial number $\tilde{e}_{i_0 j_0} = e_{ij}$ and compute a temporary potential $\tilde{p}_{i_0 j_0}$ in terms of the following four cases:

If lattice site (i_0, j_0) is not occupied by a pedestrian and is in the horizontal or vertical directions then

$$\tilde{p}_{i_0 j_0} = p_{ij} + \left(1 + \lambda / d_{e_{ij}}\right); \tag{2}$$

if lattice site (i_0, j_0) is occupied by a pedestrian and is in the horizontal or vertical directions then

$$\tilde{p}_{i_0 j_0} = p_{ij} + (1+\alpha)\left(1 + \lambda / d_{e_{ij}}\right); \tag{3}$$

if lattice site (i_0, j_0) is not occupied by a pedestrian and is in a diagonal direction then

$$\tilde{p}_{i_0 j_0} = p_{ij} + \left(1 + \beta + \lambda / d_{e_{ij}}\right); \tag{4}$$

and if lattice site (i_0, j_0) is occupied by a pedestrian and is in a diagonal direction then

$$\tilde{p}_{i_0 j_0} = p_{ij} + (1+\alpha)\left(1 + \beta + \lambda / d_{e_{ij}}\right). \tag{5}$$

Step 8. For each lattice site (i_0, j_0) evaluated according to the temporary exit serial number and potential in Step 7, its potential $p_{i_0 j_0}$ takes the minimum value among all its temporary potentials, its exit serial number $e_{i_0 j_0}$ takes the temporary exit serial number value corresponding to the minimum temporary potential, and it is added into the set of lattices that need to be checked.

Step 9. For each k $(=1, 2, \cdots, n)$, set $d_k \leftarrow d_k + \tilde{m}_k$, where $\tilde{m}_k$ is the number of lattice sites, which are added into the set of lattices that need to be checked in Step 8, satisfy $e_{ij} = k$ and are not occupied by pedestrians.

Step 10. Set $\delta \leftarrow \delta + 1$.

Step 11. If the potential of each lattice site has been determined then stop; otherwise, return to Step 7.

For each of iteration, an interval $[\delta, \delta+1)$ is determined. If the potential of a lattice site in the set of lattices that need to be checked is in the interval, then the potentials of its neighboring lattices are computed. In this way, as the parameter δ increases, more lattice potentials are computed.

Parameter d_k reflects the frontal route capacity. Intensity parameter λ (≥ 0) scales the effect of the frontal route capacity on the potential. If the potential of a lattice site is iteratively computed by the potential of the lattice sites occupied by exit k, parameter d_k records the number of empty lattice sites on the frontal routes of the lattice site to exit k. The frontal route of a lattice site comprises those lattice sites whose potential computation precedes the potential computation of the lattice site and whose potentials are used to compute the potential of the lattice site. d_k occurs in formulae (2)-(5) as a denominator and hence its initial value takes the number of lattice sites occupied by exit k to guarantee $d_k \neq 0$. Formulae (2) to (5) indicate that the potential is inversely proportional to the number of empty lattice sites on the frontal routes. When there is more free space in front of a lattice site, the increase rate of the lattice site's potential is smaller. Moreover, for each of iteration, the size of the interval $[\delta, \delta+1)$ is fixed as one. Thus, the potential of more lattice sites in the space is computed using the potential of the lattice sites occupied by the exit, near which there are more free space. If the potential of a lattice site is computed by the potential of the lattice sites occupied by an exit, then the pedestrian in the lattice site almost moves towards the exit.

Intensity parameter α (≥ 0) scales the effect of local pedestrian congestion on the potential. It indicates that the increase rate of the potential of a lattice site occupied by a pedestrian is not less than that of an unoccupied lattice site. The pedestrian space is

discretized into two-dimensional square lattices, and hence the distance of a lattice site to a neighboring lattice site in the vertical or horizontal directions is smaller than the distance of the lattice site to a neighboring lattice site in a diagonal direction. The distance between two neighboring lattice sites is reflected by terms 1 and $(1+\beta)$ in the right parenthesis of formulae (2)-(5). Intensity parameter β ($\in[0,1]$) scales the increase rate of the potential of a neighboring lattice site in a diagonal direction. It indicates that the increase rate of the potential of a neighboring lattice site in a diagonal direction is not less than that of a neighboring lattice site in the vertical or horizontal directions. A detailed description of the potential algorithm run is shown in Appendix A1.

When parameter $\lambda=0$, the algorithm degenerates into those in [18] and [21]. Furthermore, when parameters $\lambda=0$ and $\alpha=0$, the algorithm is similar to those in [16] and [17]. Contrary to the algorithm in [20], in which capacity is reflected in the link widths, capacity in the potential algorithm is reflected in the frontal free space. Section 3 shows that the algorithm can be used to reproduce more route choice modes in a scenario compared with these algorithms in [16-18, 20, 21].

When the potential algorithm is used to simulate pedestrian evacuation from a facility, the potential distribution in the space needs to be recomputed in each time step. The potential algorithm is a flood fill algorithm that can be run quickly enough in principle.

3. Numerical Results

We then simulate pedestrian route choices in a scenario shown in figure 1. In the scenario, the area of a building is discretized into 50×50 lattice sites, including those

occupied by walls. Two exits with the same widths as two lattice sites are located in the middle of the north and south walls, respectively. At the initial time, 384 pedestrians distributed throughout the lattice sites are marked as red circles. There are two obstacles denoted by shaded rectangles in the scenario. The building's link widths are the same (eight lattice sites) and the widths of the two exits are equal. Thus, if the capacity is reflected by the link widths, in line with [20], the ratios of pedestrians selecting each exit cannot be controlled by adjusting the intensity parameter of scaling capacity. We use the proposed model to simulate pedestrian evacuation in the scenario.

Place Figure 1 about here

The sensitivity parameter in formula (1) is $\varepsilon = 2$ and the intensity parameter is $\beta = \sqrt{2} - 1$. By adjusting intensity parameters α and λ, we observe the variation trend of the route choices of these pedestrians. Figure 2 shows snapshots of pedestrian evacuation in the scenario at time steps $T = 50$, 100 and 150, when $\lambda = 0$ and $\alpha = 0$, 5 and 10. When $\lambda = 0$ and $\alpha = 0$, the proposed model is similar to those in [16] and [17]. In this case, almost all pedestrians select exit 1. When $\lambda = 0$, the proposed model degenerates into those in [18] and [21]. When parameter α increases, the number of pedestrians selecting exit 1 decreases and the number of pedestrians selecting exit 2 increases. This trend can also be seen in figure 3, which displays the potentials of lattices in the scenario at time steps $T = 50$, 100 and 150 when $\lambda = 0$ and $\alpha = 0$, 5 and 10. Pedestrians move along the direction in which the potential decreases. For each α value, the apex of the potential is still closer to exit 1. Thus, for each α value, the number of pedestrians selecting exit 1 is more than the number of pedestrians selecting exit 2. In fact, when parameter α increases, the number of pedestrians selecting exit 1 cannot decrease to less than the number of pedestrians

selecting exit 2. This can be observed in figure 4.

Place Figure 2 about here

Place Figure 3 about here

Figure 4 shows the relation of the number of evacuation time steps of each exit and number of pedestrians evacuating from each exit to parameter α, varying from 0 to 15 for the scenario in the case of $\lambda = 0$. The number of evacuation time steps of each exit refers to the number of time steps needed for all pedestrians to leave the building, i.e., the number of evacuation time steps of the last pedestrian to leave the building through the exit. Twenty simulations are conducted for each parameter value, and the number of time steps and number of pedestrians are the averages across 20 simulations. As the α value increases, both the number of time steps of exit 1 and the number of pedestrians evacuating from exit 1 decline and the decline rates decrease. For exit 2, both the number of time steps and the number of pedestrians rise and the rise rates decrease. Moreover, the number of time steps of exit 1 is still larger than that of exit 2 and the number of pedestrians evacuating from exit 1 is more than that of pedestrians evacuating from exit 2. Hence, for these models in [16-18, 21], the ratios of pedestrians selecting each exit cannot be adjusted so that the evacuation time of exit 1 and number of pedestrians evacuating from exit 1 are less than those for exit 2.

Place Figure 4 about here

Figure 5 shows snapshots of pedestrian evacuation in the scenario at time steps 50, 100 and 150 when $\alpha = 1$ and $\lambda = 0$, 17.5 and 30. As parameter λ increases, the

number of pedestrians evacuating from exit 1 decreases and the number of pedestrians evacuating from exit 2 increases. When $\lambda = 0$, there are still pedestrians near exit 1 at time step 150, and there is only one individual near exit 2. As a result, the evacuation time of exit 1 is larger than that of exit 2. When $\lambda = 30$, the number of pedestrians near exit 1 is less than the number of pedestrians near exit 2 at time step 15, and the evacuation time of exit 1 is less than that of exit 2. This phenomenon can also be observed in figure 6, which shows lattice potentials in the scenario at time steps 50, 100 and 150 when $\alpha = 1$ and $\lambda = 0$, 17.5 and 30. As parameter λ increases, the apex of the potential moves from a location closer to exit 1 to one closer to exit 2 at time step 150.

Place Figure 5 about here

Place Figure 6 about here

Figure 7 shows the relation of the number of evacuation time steps of each exit and number of pedestrians evacuating from each exit to parameter λ, varying from 0 to 30 for the scenario when $\alpha = 1$. When $\lambda = 0$, the number of evacuation time steps of exit 1 is larger than that of exit 2. As parameter λ increases, the number of evacuation time steps of exit 1 decreases and that of exit 2 increases. When $\lambda = 17.5$, the numbers of evacuation time steps of the two exits are almost equal. For those λ values larger than 17.5, the number of evacuation time steps of exit 1 becomes smaller than that of exit 2. A similar phenomenon can be observed for the number of pedestrians evacuating from each exit. Therefore, the proposed model can reproduce more route choice modes in a scenario than these models in [16-18, 20, 21] and is more likely to be used to reproduce real pedestrian route choice behavior.

Place Figure 7 about here

4. Experiment Description and Results

In this section, we introduce three groups of pedestrian evacuation experiments and try to reproduce pedestrian route choice behavior using the proposed model.

The three groups of experiments were conducted in a classroom, which is illustrated schematically in figure 8. The size of the classroom was 5.65×10.80 m^2. Two exits with widths of 0.76 m and 1.05 m were located in the north wall close to the west and east walls, respectively. Two obstacles, a lectern and a computer workbench, were placed on the west side of the classroom. Seventy pairs of desks and chairs were arranged in eight rows of nine. The obstacles and the desks are denoted in the schema by light grey rectangles, and the initial positions of individuals are denoted by green circles numbered 1 to 70. The desks and chairs were divided into three sections by two horizontal aisles. The transverse distance between desks in each section was 0.9 m. The vertical width of the desks was 1.36 m in the north section, 2.06 m in the middle section and 1.23 m in the south section. The width of each of the horizontal aisles was 0.5 m. The chairs folded automatically, so when individuals stood up, the chairs folded up and left space for the individuals to move between the desks. A video camera was mounted at the southwest corner of the classroom and was used to record the evacuation processes.

Place Figure 8 about here

Three groups of experiments were carried out, in which 10, 20 and 30 students were asked to perform 8, 8 and 16 evacuation processes, respectively. In each evacuation

process, the initial positions of the students were randomly generated using a computer. All individuals stood up from their seats and moved towards the exits as soon as the command to evacuate was given. Once they arrived at the exits, they left the classroom and then their initial positions, the exits they selected and their evacuation times were recorded. An individual's evacuation time is defined as the time that elapsed between when the command to evacuate was given and the moment the individual exited the classroom. Let Experiment i-j represent the jth evacuation process in the ith group of experiments. The individuals' initial positions, exit selections and evacuation times are given in Tables 1-3 (see Appendix A2). Figure 9 shows photographs of individuals evacuating the classroom in Experiment 1-2 at 0 and 5 s, Experiment 2-2 at 0 and 5 s and Experiment 3-4 at 0 and 5 s.

Place Figure 9 about here

To reproduce the exit choice behavior of the individuals in these experiments using the proposed model, we discretized the classroom into 12×27 lattice sites according to space distribution. A schematic illustration of the classroom in these simulations is shown in figure 10. We let Simulation i-j represent the jth evacuation process in the ith group of simulation. The number of individuals and their initial positions in Simulation i-j are identical to those in Experiment i-j. We compare the numbers of individuals evacuating from each exit and the evacuation times at each exit obtained in both Experiment i-j and Simulation i-j. Twenty simulations are conducted for each Simulation i-j and the number of time steps and number of pedestrians are the averages across the 20 simulations.

Place Figure 10 about here

In these simulations, the sensitivity parameter in formula (1) is $\varepsilon = 2$ and the intensity parameters are $\beta = \sqrt{2} - 1$ and $\alpha = 1$. Let the parameter λ vary from 0 to 50 with an interval of 1. The following indications, I_1 and I_2, are used to evaluate the degree of similarity between the numbers and times obtained in these simulations and experiments.

$$I_1 = \sum_i \sum_j \sum_k \left(\bar{N}_{ijk} - \tilde{N}_{ijk} \right)^2, \tag{6}$$

where $\bar{N}_{ijk}$ and $\tilde{N}_{ijk}$ are the numbers of individuals evacuating from exit k $(=1,2)$ in Experiment i-j and Simulation i-j, respectively.

$$I_2 = \sum_i \sum_j \sum_k \left(t_{ijk} - S_{ijk} \Delta t \right)^2, \tag{7}$$

where t_{ijk} is the evacuation time of exit k $(=1,2)$ in Experiment i-j and S_{ijk} is the number of evacuation time steps of exit k $(=1,2)$ in Simulation i-j. The time step Δt is computed by

$$\Delta t = \frac{\sum_i \sum_j \sum_k t_{ijk} S_{ijk}}{\sum_i \sum_j \sum_k S_{ijk}^2}; \tag{8}$$

that is to say,

$$\Delta t = \arg\min_{x \geq 0} \sum_i \sum_j \sum_k \left(t_{ijk} - S_{ijk} x \right)^2. \tag{9}$$

Smaller I_1 or I_2 values indicate simulations that can reproduce these experiments more effectively.

Figure 11 shows the relation of indications I_1 and I_2 to parameter λ. As parameter λ increases, both indications I_1 and I_2 first decline and then rise. Moreover, both indications I_1 and I_2 take minimum values at about $\lambda = 12$. When $\lambda = 12$, the corresponding time step $\Delta t = 0.44$. This implies a free walking speed of approximately 1.1 m/s, which is very close to the findings of many observational studies [29, 30]. Figures 12 and 13 compare the numbers of individuals evacuating from each exit and the evacuation times at each exit between the experiments and

simulations, when $\lambda = 12$. For either the numbers or times, these points are on or near the diagonal lines. Therefore, the proposed model can be used to formulate pedestrian route choice behavior in the three groups of experiments.

Place Figure 11 about here

Place Figure 12 about here

Place Figure 13 about here

5. Conclusions

We propose an algorithm for the potential field that navigates pedestrian route choice in the individual-based model to simulate the evacuation process of pedestrians from a facility. The potential field measures three factors that affect the route choice, including route distance, pedestrian congestion and route capacity. These models in [16-18, 21] are special cases of the proposed model. In this model, route capacity is reflected by the free space in front of each individual, which is different to the method used in [20]. Through numerical simulation, we show that the proposed model can formulate more route choice modes in a scenario compared with these models in [16-18, 20, 21]. Therefore, it is more likely to be used to reproduce real pedestrian route choice behavior. In addition, the model avoids several issues that exist in those in [19, 22, 23, 25, 26].

We also conduct three groups of experiments, in which individuals evacuate a classroom, and compare experiment results and model simulations. Experimental and numerical results indicate that the model can reproduce pedestrian route choice more

effectively. Thus, it is helpful for devising evacuation schemes and designing internal layouts and exit arrangements in buildings similar to the classroom.

In addition, the proposed potential field algorithm is extendable to other areas. It may be used to consider pedestrian route choices in individual-based models with continuous space representation and vehicle route choices in urban networks. Further, it may be applied to autonomous robot navigation, providing solutions for a robot's path-finding issues.

Acknowledgments

The work described in this paper was jointly supported by grants from the National Natural Science Foundation of China (71001047 and 71261016), the National Basic Research Program of China (2012CB725401) and the Research Grants Council of the Hong Kong Special Administrative Region, China (HKU7184/10E), and program for Young Talents of Science and Technology in Universities of Inner Mongolia Autonomous Region (NJYT-12-B04).

Appendix

A.1. Flow chart of potential algorithm

Figure 14 presents the flow chart of the potential algorithm. In this figure, p_{ij}, o_{ij}, e_{ij}, $\tilde{p}_{ij}$, n, d_k $(k=1,2,\cdots,n)$, δ, λ, α, and β have the same meaning with those in Section 2. n_t is the total number of lattice sites in the closed areas, and is used to determine whether the potentials of all lattice sites are computed, i.e., whether the algorithm stops. n_o is the number of lattice sites occupied by a wall or obstacle, and the $n_o \times 2$ dimensional array S_o records the coordinates of these lattice sites.

n_e^i is the number of lattice sites occupied by exit i, and the $n_e^i \times 2$ dimensional array S_e^i records the coordinates of these lattice sites. n_n^i is the number of lattice sites that have a neighboring lattice site occupied by exit i in the horizontal or vertical directions, and the $n_n^i \times 2$ dimensional array S_n^i records the coordinates of these lattice sites. n_c is the number of lattice sites that need to be checked, and the $n_c \times 2$ dimensional array S_c records the coordinates of these lattice sites. S_1 and S_2 are two arrays that record the coordinates of n_1 and n_2 lattice sites, respectively, and they are used to update the array S_c. The 8×2 dimensional array S_{ij} records the coordinates of eight lattice sites adjacent to lattice site (i, j), and the coordinates of these lattice sites in horizontal and vertical directions (diagonal directions) are recorded in odd lines (even lines).

Place Figure 14 about here

A.2. Evacuation Times and Exit Choices of Pedestrians in These Experiments

See Tables 1 to 3.

Place Table 1 about here

Place Table 2 about here

Place Table 3 about here

References

[1] Burstedde C, Klauck K, Schadschneider A and Zittartz J, *Simulation of pedestrian*

dynamics using a two-dimensional cellular automaton, 2001 *Physica* A **295** 507

[2] Hughes R L, *A continuum theory for the flow of pedestrians*, 2002 *Transp. Res.* B **36** 507

[3] Antonini G, Bierlaire M and Weber M, *Discrete choice models of pedestrian walking behavior*, 2006 *Transp. Res.* B **40** 667

[4] Seyfried A, Passon O, Steffen B, Boltes M, Rupprecht T and Klingsch W, *New insights into pedestrian flow through bottlenecks*, 2009. *Transp. Sci.* **43** 395

[5] Helbing D, Farkas I and Vicsek T, *Simulating dynamical features of escape panic*, 2000 *Nature* **407** 487

[6] Huang L, Wong S C, Zhang M, Shu C W and Lam W H K, *Revisiting Hughes' dynamic continuum model for pedestrian flow and the development of an efficient solution algorithm*, 2009 *Transp. Res.* B **43** 127

[7] Lin P, Lo S M, Huang H C and Yuen K K, *On the use of multi-stage time-varying quickest time approach for optimization of evacuation planning*, 2008 *Fire Safety J.* **43** 282

[8] Cepolina E M, *Phased evacuation: an optimisation model which takes into account the capacity drop phenomenon in pedestrian flows*, 2009 *Fire Safety J.* **44** 532

[9] Pursals S C and Garzón F G, *Optimal building evacuation time considering evacuation routes*, 2009 *Eur. J. Oper. Res.* **192** 692

[10] Höcker M, Berkhahn V, Kneidl A, Borrmann A and Klein W, *Graph-based approaches for simulating pedestrian dynamics in building models*, 2010 *ECPPM 2010 – eWork and eBusiness in Architecture, Engineering and Construction* ed K Menzel and R Scherer (Leiden: CRC Press) pp 389–394

[11] Kneidl A and Borrmann A, *How do pedestrians find their way – results of an experimental study with students compared to simulation results*, 2011 *Emergency Evacuation of people from Buildings* ed W Jaskólowski and P Kepka

[12] Wagoum A U K, Seyfried A and Holl S, Modeling the dynamics route choice of pedestrians to assess the criticality of building evacuation, 2012 Adv. Complex Syst. **15** 1250029

[13] Hoogendoorn S P and Bovy P H L, *Simulation of pedestrian flows by optimal control and differential games*, 2003 *Optim. Contr. Appl. Met.* **24** 153

[14] Hoogendoorn S P and Bovy P H L, *Pedestrian route-choice and activity scheduling theory and models*, 2004 *Transp. Res.* B **38** 169

[15] Asano M, Iryo T and Kuwahara M, Microscopic pedestrian simulation model combined with a tactical model for route choice behaviour, 2010 *Transp. Res.* C **18** 842

[16] Varas A, Cornejo M D, Mainemer D, Toledo B, Rogan J, Munoz V and Valdivia J A, *Cellular automaton model for evacuation process with obstacles*, 2007 *Physica* A **382** 631

[17] Huang H J and Guo R Y, *Static floor field and exit choice for pedestrian evacuation in rooms with internal obstacles and multiple exits*, 2008 *Phys. Rev.* E **78** 021131

[18] Kretz T, *Pedestrian traffic: on the quickest path*, 2009 *J. Stat. Mech.* P03012

[19] Guo R Y and Huang H J, *Logit-based exit choice model of evacuation in rooms with internal obstacles and multiple exits*, 2010 *Chin. Phys.* B **19** 030501

[20] Guo R Y and Huang H J, *Route choice in pedestrian evacuation: formulated using a potential field*, 2011 *J. Stat. Mech.* P04018

[21] Hartmann D, *Adaptive pedestrian dynamics based on geodesics*, 2010 *New J. Phys.* **12** 043032

[22] Zhao H and Gao Z Y, *Reserve capacity and exit choosing in pedestrian evacuation dynamics*, 2010 *J. Phys. A: Math. Theor.* **43** 105001

[23] Alizadeh R, *A dynamic cellular automaton model for evacuation process with obstacles*, 2011 *Safety Sci.* **49** 315

[24] Guo R Y, Huang H J and Wong S C, *Route choice in pedestrian evacuation under conditions of good and zero visibility: experimental and simulation results*, 2012 *Transp. Res.* B **46** 669

[25] Xu Y and Huang H J, *Simulation of exit choosing in pedestrian evacuation with consideration of the direction visual field*, 2012 *Physica* A **391** 991

[26] Zhang P, Jian X X, Wong S C and Choi K, *Potential field cellular automata model for pedestrian flow*, 2012 *Phys. Rev.* E **85** 021119

[27] Muramatsu M, Irie T and Nagatani T, *Jamming transition in pedestrian counter flow*, 1999 *Physica* A **267** 487

[28] Kirchner A and Schadschneider A, Simulation of evacuation processes using a bionics-inspired cellular automaton model for pedestrian dynamics, 2002 *Physica* A **312** 260

[29] Seyfried A., Steffen B, Klingsch W and Boltes M, *The fundamental diagram of pedestrian movement revisited*, 2005 *J. Stat. Mech.* P10002

[30] Wong S C, Leung W L, Chan S H, Lam W H K, Yung N H C, Liu C Y and Zhang P, *Bidirectional pedestrian stream model with oblique intersecting angle*, 2010 *J. Transp. Eng.* **136** 234

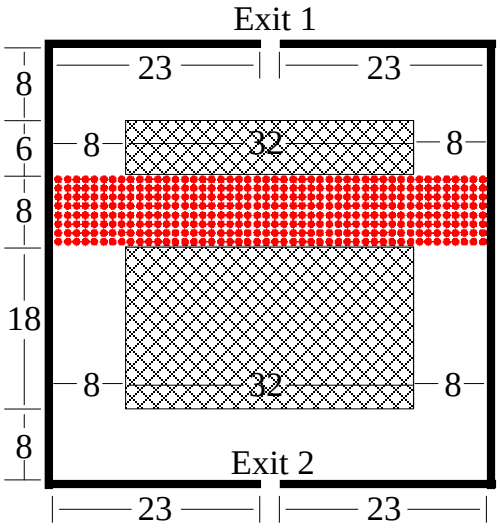

Figure 1. Simulation scenario (unit of size: lattice site).

Figure 2. Snapshots of pedestrian evacuation in the figure 1 scenario at time steps 50, 100 and 150 when $\lambda = 0$ and $\alpha = 0$, 5 and 10.

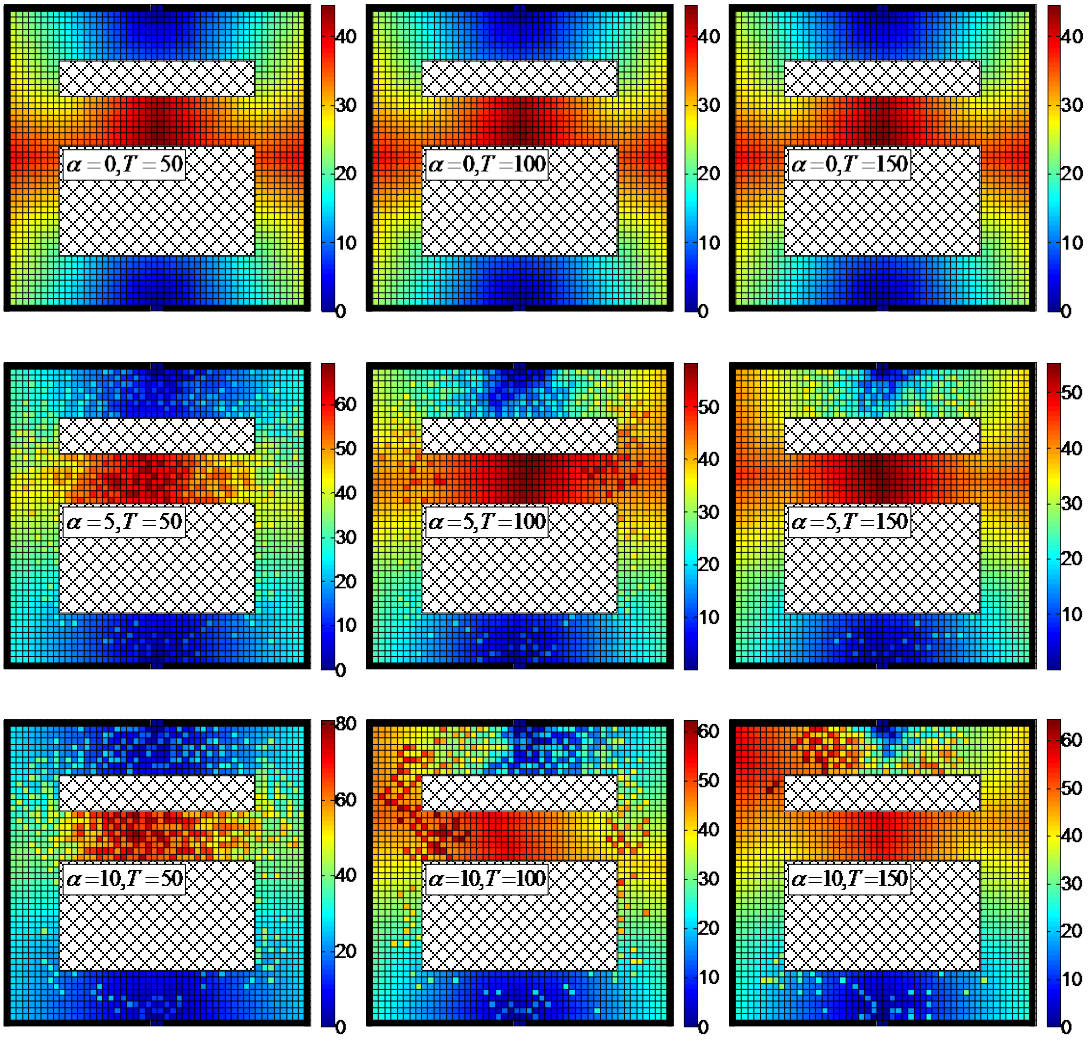

Figure 3. Potential of lattices in the figure 1 scenario at time steps 50, 100 and 150 when $\lambda = 0$ and $\alpha = 0$, 5 and 10.

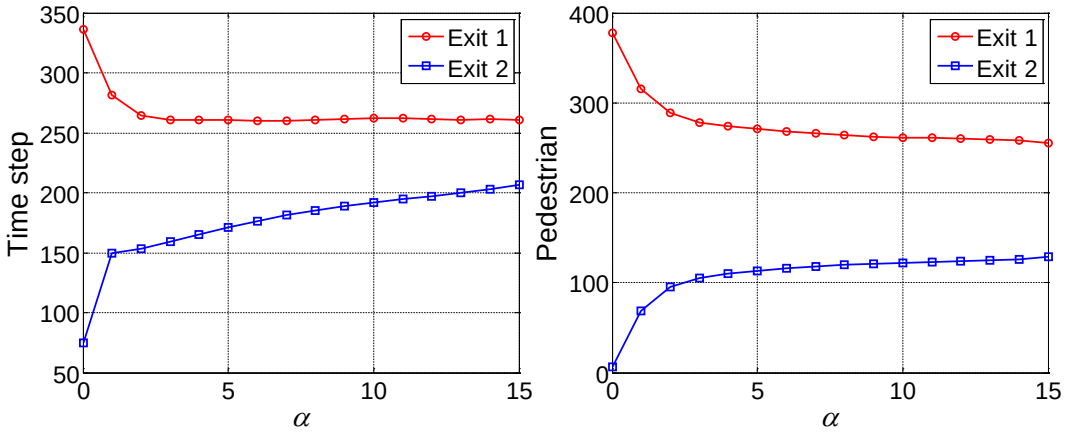

Figure 4. Relation of the number of evacuation time steps of each exit and number of pedestrians evacuating from each exit to parameter α for the figure 1 scenario when $\lambda = 0$.

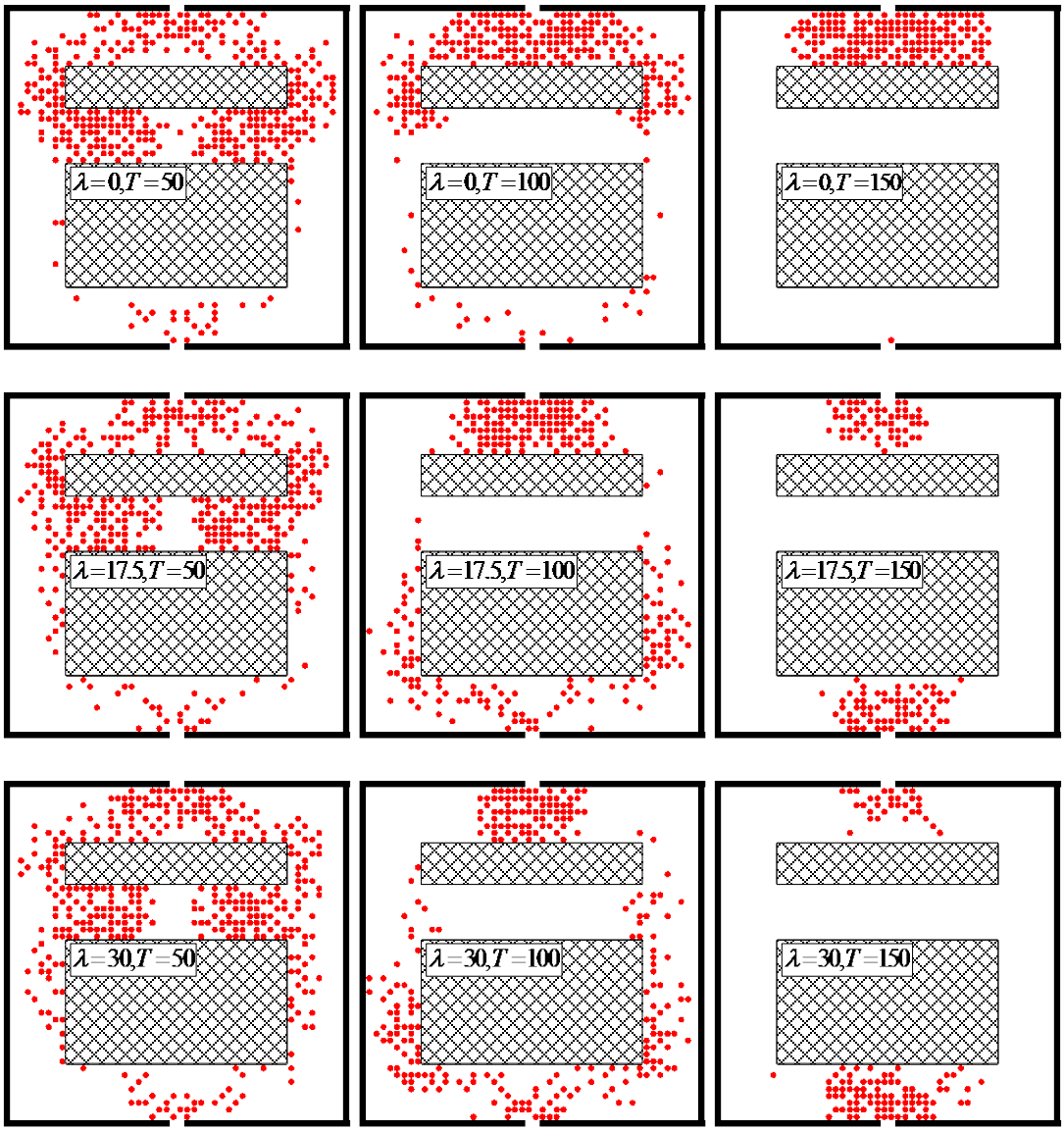

Figure 5. Snapshots of pedestrian evacuation in the figure 1 scenario at time steps 50, 100 and 150 when $\alpha = 1$ and $\lambda = 0$, 17.5 and 30.

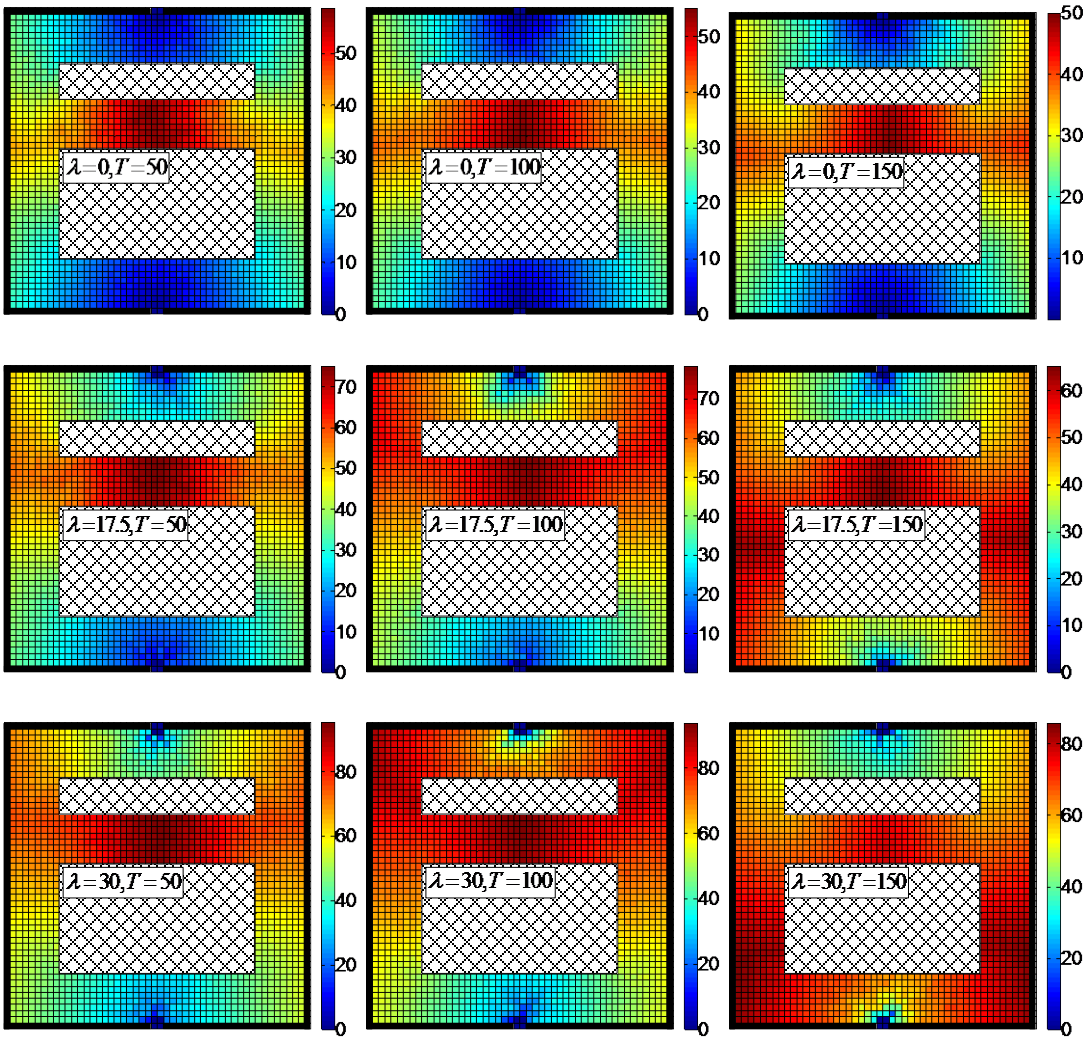

Figure 6. Potential of lattices in the figure 1 scenario at time steps 50, 100 and 150 when $\alpha = 1$ and $\lambda = 0$, 17.5 and 30.

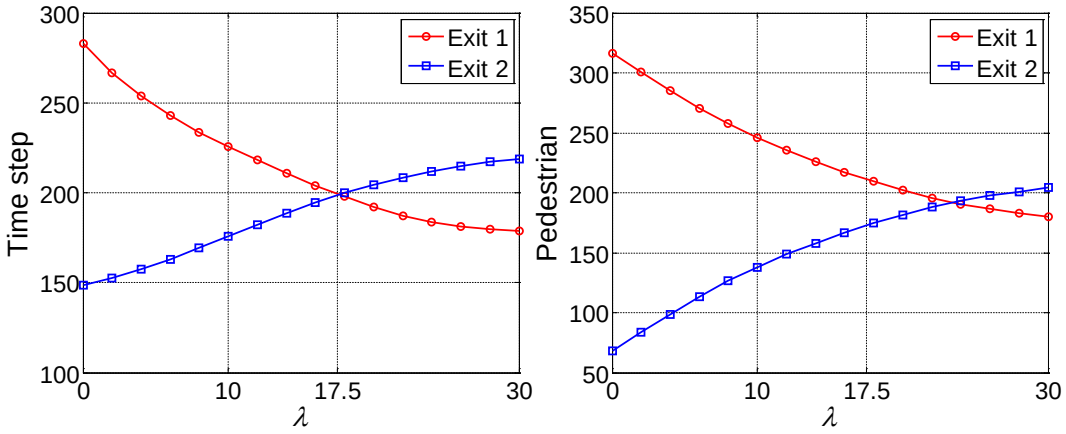

Figure 7. Relation of the number of evacuation time steps of each exit and number of pedestrians evacuating from each exit to parameter λ for the figure 1 scenario when $\alpha = 1$.

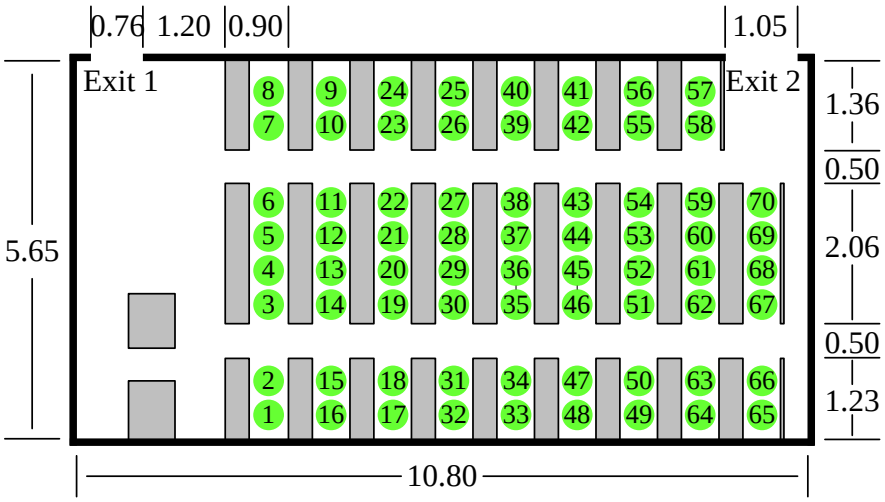

Figure 8. Schematic illustration of the classroom used in the experiments (unit of size: m).

Figure 9. Photographs of pedestrian evacuation from the classroom in Experiment 1-2 at 0 and 5 s, Experiment 2-2 at 0 and 5 s, and Experiment 3-4 at 0 and 5 s.

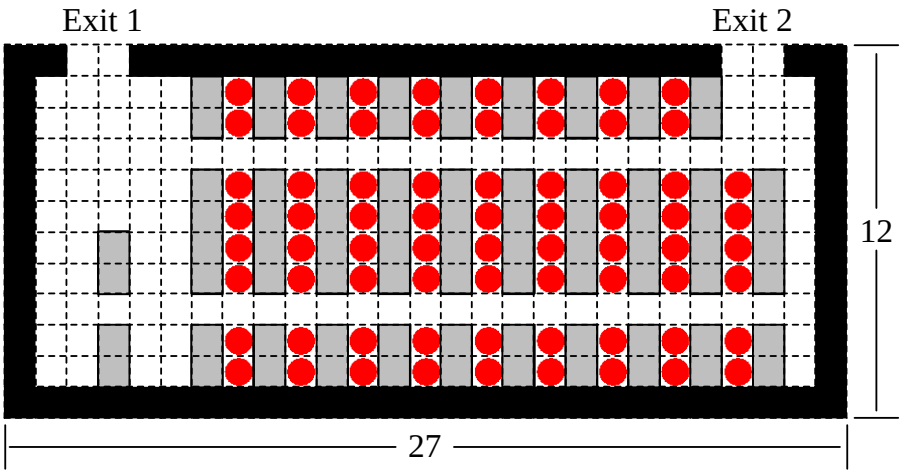

Figure 10. Schematic illustration of the classroom in the simulations (unit of size: lattice site).

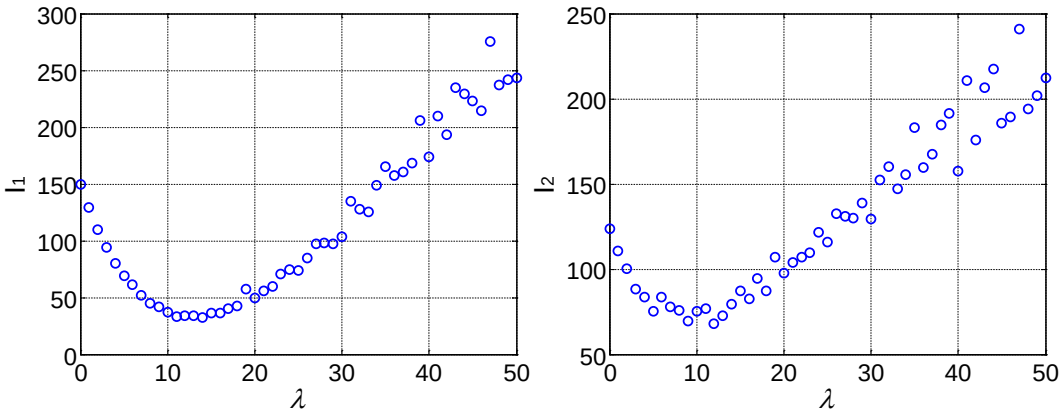

Figure 11. Relation of indications I_1 and I_2 to parameter λ for the figure 10 scenario when $\varepsilon = 2$, $\beta = \sqrt{2} - 1$, and $\alpha = 1$.

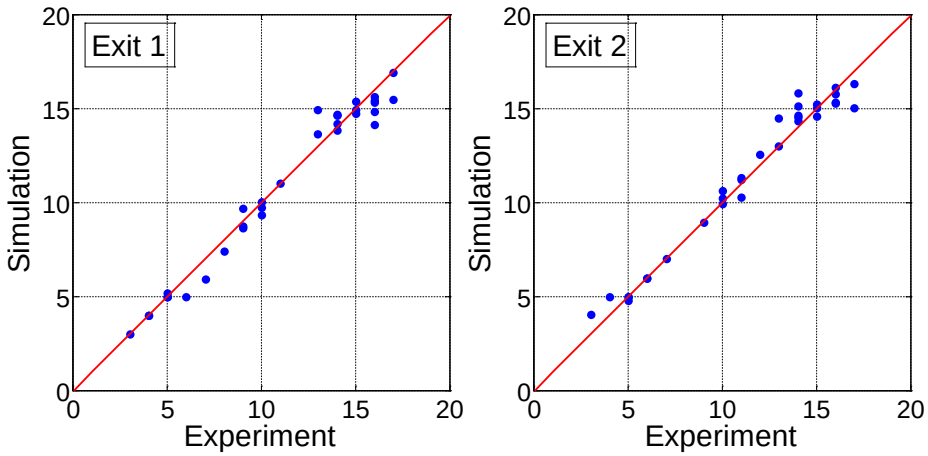

Figure 12. Numbers of pedestrians evacuating from each exit in the experiments and those in the simulations.

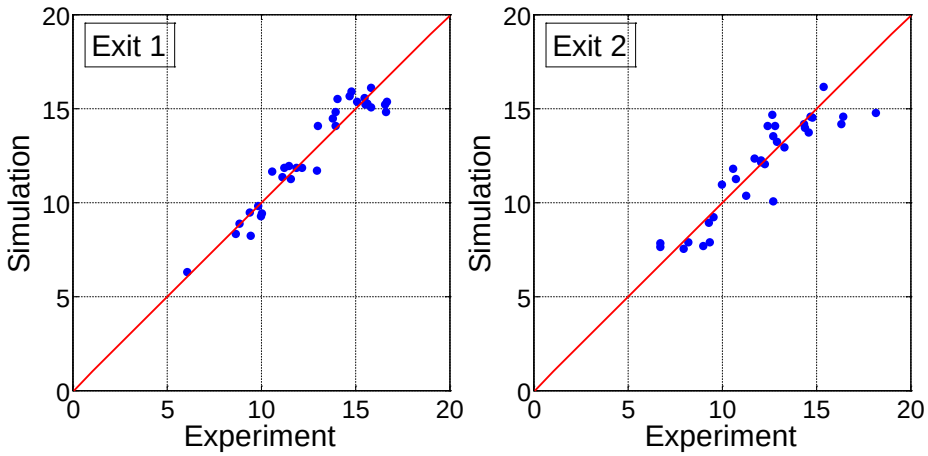

Figure 13. Evacuation times of each exit in the experiments and those in the simulations.

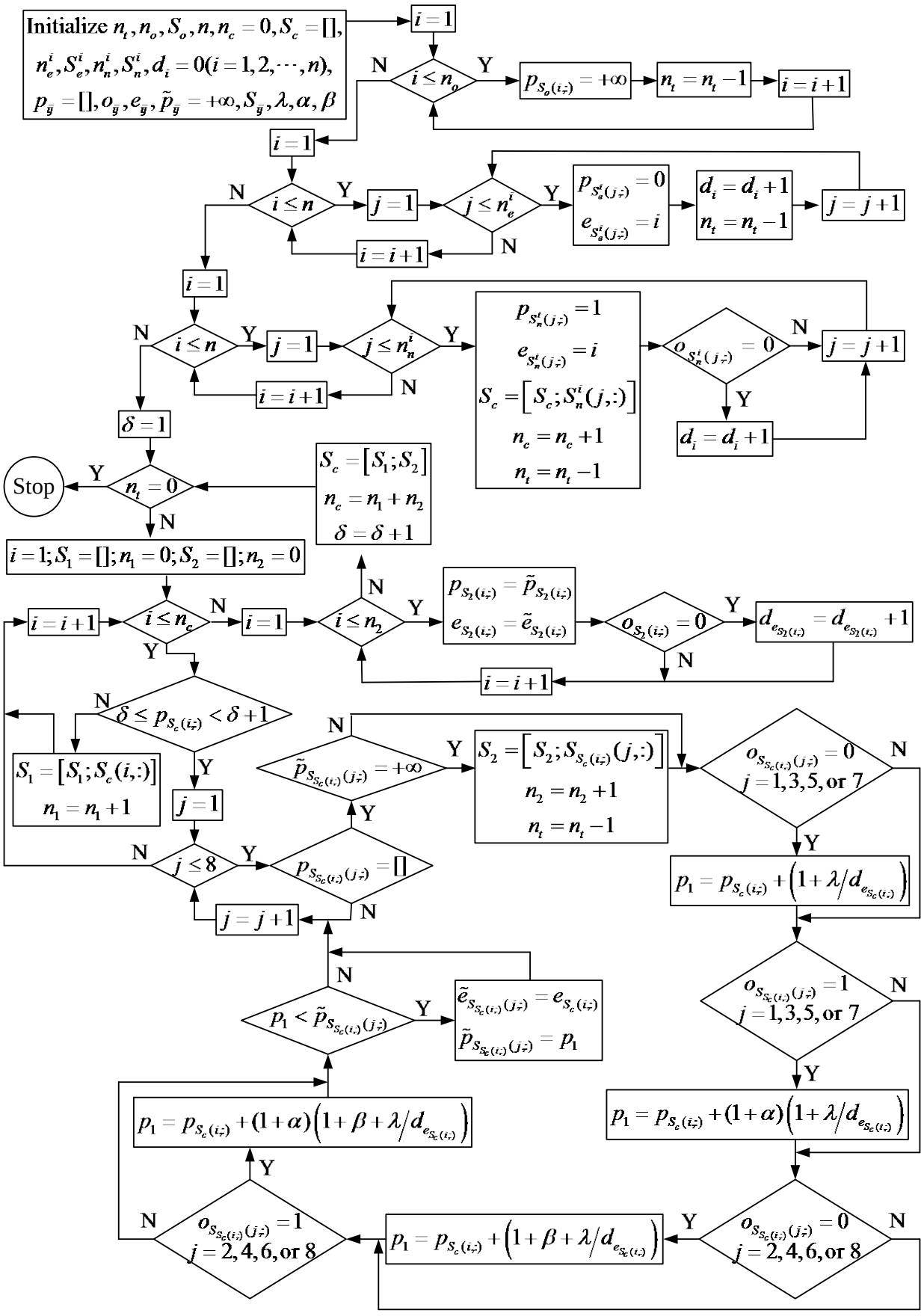

Figure 14. Flow chart of the potential algorithm.

Table 1 Evacuation times (unit: s) and exit choices of pedestrians in Experiments 1-1 to 1-8.

Experiment 1-1			Experiment 1-2			Experiment 1-3			Experiment 1-4		
Position	Exit	Time	Position	Exit	Time	Position	Exit	Time	Position	Exit	Time
3	1	6.57	7	1	4.90	3	1	6.63	2	1	6.87
9	1	5.52	13	1	6.36	5	1	3.64	15	1	7.74
13	1	7.52	24	1	7.39	10	1	4.65	18	1	8.53
20	1	8.59	25	1	8.66	13	1	5.69	22	1	5.64
38	2	8.32	32	1	9.82	27	1	7.57	31	1	9.37
47	2	9.32	35	2	7.47	30	1	10.01	34	2	8.15
52	2	5.10	37	2	6.61	35	1	8.74	40	2	5.94
57	2	3.71	41	2	5.65	44	2	4.82	52	2	4.76
64	2	7.26	44	2	4.60	45	2	6.68	63	2	6.97
66	2	6.37	51	2	9.52	69	2	3.04	69	2	2.82
Experiment 1-5			Experiment 1-6			Experiment 1-7			Experiment 1-8		
Position	Exit	Time	Position	Exit	Time	Position	Exit	Time	Position	Exit	Time
6	1	5.59	4	1	4.67	11	1	3.86	12	1	4.38
7	1	4.40	8	1	3.62	19	1	7.84	16	1	9.96
12	1	6.60	13	1	6.04	27	1	5.69	24	1	5.95
20	1	8.52	42	2	5.67	30	1	8.79	25	1	6.80
21	1	7.69	51	2	8.97	37	2	5.64	31	1	7.96
37	1	9.42	52	2	6.58	44	2	7.41	45	2	7.27
45	2	5.95	60	2	3.94	47	2	8.34	48	2	7.93
55	2	4.51	66	2	7.93	48	2	9.25	56	2	6.34
56	2	6.67	67	2	4.96	56	2	3.83	61	2	4.54
57	2	3.26	70	2	2.77	70	2	2.02	67	2	5.42

Table 2 Evacuation times (unit: s) and exit choices of pedestrians in Experiments 2-1 to 2-8.

Experiment 2-1			Experiment 2-2			Experiment 2-3			Experiment 2-4		
Position	Exit	Time	Position	Exit	Time	Position	Exit	Time	Position	Exit	Time
4	1	7.77	7	1	4.35	3	1	5.66	3	1	6.34
6	1	5.13	16	1	7.84	8	1	4.91	6	1	3.24
8	1	4.05	20	1	9.29	14	1	7.20	15	1	7.08
9	1	6.99	25	1	8.71	19	1	7.94	16	1	9.40
13	1	8.65	28	1	6.48	23	1	6.33	25	1	10.25
18	1	9.48	31	1	10.59	30	1	9.39	26	1	5.49
25	1	11.38	35	1	11.45	31	1	10.27	27	1	7.86
31	1	10.56	39	1	9.96	32	1	11.09	28	1	8.64
32	1	12.93	42	2	11.69	39	1	8.67	36	2	11.34
33	2	12.70	43	2	5.73	41	2	10.55	40	1	11.17
39	1	12.09	52	2	10.26	42	2	8.89	41	2	10.34
41	2	9.60	53	2	9.24	43	2	8.01	49	2	12.01
49	2	11.65	55	2	3.60	45	2	9.06	53	2	8.51
51	2	10.61	56	2	8.35	46	2	12.22	54	2	5.62
53	2	8.70	61	2	5.29	52	2	11.35	55	2	7.58
58	2	3.61	63	2	6.74	53	2	6.26	56	2	9.39
59	2	5.70	64	2	10.93	58	2	5.44	57	2	3.75
60	2	6.73	65	2	6.25	60	2	4.47	63	2	6.28
66	2	7.81	67	2	4.38	61	2	6.85	65	2	6.80
70	2	4.78	69	2	3.39	67	2	3.47	67	2	4.71
Experiment 2-5			Experiment 2-6			Experiment 2-7			Experiment 2-8		
Position	Exit	Time	Position	Exit	Time	Position	Exit	Time	Position	Exit	Time
2	1	5.39	3	1	5.40	1	1	6.52	4	1	5.87
8	1	3.80	4	1	8.58	3	1	7.25	8	1	5.27
12	1	6.84	6	1	4.68	6	1	4.15	13	1	6.68
13	1	8.36	7	1	3.66	8	1	4.95	16	1	7.64
15	1	6.17	13	1	6.06	11	1	5.65	19	1	9.04
20	1	7.58	16	1	7.74	15	1	8.28	20	1	8.40
25	1	10.57	18	1	10.35	18	1	9.52	25	1	9.67
29	1	9.80	21	1	6.93	21	1	9.05	29	2	10.53
30	1	9.03	27	1	9.41	25	1	10.29	31	1	10.40
33	2	10.5	30	1	11.24	32	1	11.54	34	1	11.04
36	2	9.14	31	1	12.11	39	2	9.93	37	1	11.82
44	2	8.34	33	2	10.67	42	2	9.31	38	2	7.24
47	2	9.70	37	2	9.20	49	2	8.16	44	2	6.39
48	2	11.26	39	2	7.43	51	2	8.69	45	2	8.79
54	2	6.72	40	2	9.87	55	2	4.82	48	2	9.57

57	2	4.19	47	2	7.98	56	2	7.58	53	2	4.82
60	2	5.12	52	2	6.75	57	2	6.83	55	2	3.84
61	2	7.61	53	2	5.30	58	2	6.06	64	2	8.04
68	2	5.92	65	2	8.51	59	2	3.83	65	2	5.54
69	2	3.22	66	2	5.95	63	2	5.43	70	2	2.00

Table 3 Evacuation times (unit: s) and exit choices of pedestrians in Experiments 3-1 to 3-16.

Experiment 3-1			Experiment 3-2			Experiment 3-3			Experiment 3-4		
Position	Exit	Time	Position	Exit	Time	Position	Exit	Time	Position	Exit	Time
1	1	10.85	1	1	8.69	6	1	4.65	2	1	6.26
4	1	4.76	2	1	5.64	7	1	3.73	4	1	6.91
8	1	3.34	3	1	7.06	8	1	2.98	9	1	7.82
11	1	5.47	9	1	4.48	11	1	5.41	10	1	4.41
13	1	7.83	12	1	6.39	13	1	6.38	11	1	5.40
15	1	6.28	16	1	10.17	15	1	7.02	14	1	8.47
16	1	13.62	19	1	10.96	16	1	11.27	16	1	9.04
18	1	9.72	22	1	7.98	18	1	13.08	17	1	10.58
23	1	7.00	28	1	9.42	19	1	9.76	23	1	9.95
25	1	11.78	31	1	13.44	20	1	12.14	26	1	11.39
27	1	8.95	32	1	12.12	21	1	10.50	28	1	12.53
29	1	12.66	33	2	15.37	22	1	7.73	30	1	13.21
30	1	14.53	34	2	14.52	26	1	8.67	31	1	12.12
32	2	16.72	35	1	12.77	35	1	13.78	35	2	14.36
36	2	15.41	36	1	14.98	36	2	14.75	38	1	13.97
37	2	12.25	39	1	15.83	41	2	12.46	39	1	14.67
41	2	11.34	41	2	10.92	42	2	10.21	40	2	11.68
43	2	10.47	42	2	10.08	44	2	13.16	42	2	9.90
44	2	13.22	44	2	8.41	45	2	13.82	43	2	10.86
48	1	16.59	45	2	12.40	50	2	10.97	48	2	13.42
51	2	18.14	46	2	13.91	52	2	8.76	49	2	12.57
54	2	6.85	48	2	13.20	54	2	5.79	50	2	8.20
56	2	9.57	50	2	11.67	57	2	4.16	53	2	6.49
57	2	5.57	51	2	6.58	60	2	4.80	56	2	9.06
60	2	4.49	54	2	3.95	61	2	6.78	58	2	4.21
62	2	7.94	56	2	4.91	62	2	9.52	59	2	2.49
63	2	8.87	60	2	3.33	64	2	11.76	61	2	7.19
64	2	11.00	62	2	7.45	65	2	7.76	66	2	4.84
66	2	14.33	64	2	9.26	69	2	3.47	67	2	5.77
68	2	3.65	65	2	5.72	70	2	2.00	68	2	3.38
Experiment 3-5			Experiment 3-6			Experiment 3-7			Experiment 3-8		
Position	Exit	Time	Position	Exit	Time	Position	Exit	Time	Position	Exit	Time
2	1	6.85	1	1	5.49	3	1	5.38	1	1	7.13
3	1	8.70	6	1	2.89	5	1	4.45	3	1	5.92
6	1	5.34	12	1	4.72	7	1	3.13	4	1	5.24
7	1	3.51	14	1	7.85	9	1	6.23	7	1	3.69
11	1	4.49	15	1	9.21	14	1	7.56	8	1	4.48

14	1	7.73	17	1	9.63	16	1	10.19	9	1	6.50
18	1	9.43	21	1	8.67	17	1	13.42	16	1	8.65
20	1	10.97	23	1	6.29	18	1	10.72	19	1	11.00
21	1	10.26	24	1	7.13	19	1	12.32	21	1	10.31
22	1	6.19	25	1	13.64	21	1	8.34	22	1	7.88
23	1	7.24	27	1	10.30	24	1	6.79	23	1	9.44
26	1	12.89	30	1	11.26	25	1	11.36	24	1	12.15
31	1	13.93	33	1	14.64	26	1	9.23	29	1	12.74
33	2	15.26	34	1	12.16	31	1	14.74	30	1	13.64
34	2	13.50	38	1	15.24	32	1	15.52	31	1	14.40
39	2	14.35	41	2	12.86	34	2	10.29	34	1	15.07
40	2	16.29	45	1	16.63	35	2	12.63	38	2	12.56
41	2	12.68	51	2	11.99	36	1	16.55	39	2	13.28
44	2	9.41	52	2	11.27	37	2	10.93	42	2	9.99
45	2	10.21	53	2	8.57	38	1	12.79	44	2	11.73
47	2	11.84	54	2	6.36	39	2	9.26	47	2	10.77
50	2	10.98	56	2	7.77	41	2	11.78	53	2	9.12
51	2	7.40	57	2	3.41	42	2	7.59	55	2	6.50
55	2	5.31	59	2	5.00	43	2	6.14	57	2	4.64
56	2	6.03	60	2	7.01	49	2	8.46	58	2	3.15
60	2	4.42	62	2	10.44	52	2	6.85	62	2	5.42
63	2	8.25	64	2	9.63	53	2	5.35	64	2	7.25
65	2	6.72	68	2	5.72	57	2	4.53	65	2	8.13
68	2	3.28	69	2	4.29	58	2	3.49	67	2	3.95
69	2	2.37	70	2	2.43	70	2	2.73	70	2	2.30

Experiment 3-9			Experiment 3-10			Experiment 3-11			Experiment 3-12		
Position	Exit	Time	Position	Exit	Time	Position	Exit	Time	Position	Exit	Time
1	1	6.20	2	1	5.80	1	1	6.91	5	1	6.15
2	1	4.75	3	1	4.24	4	1	5.52	6	1	3.96
4	1	5.39	6	1	3.12	5	1	5.01	7	1	4.84
5	1	3.26	12	1	5.04	6	1	4.32	11	1	5.46
9	1	6.88	17	1	13.96	7	1	3.52	14	1	11.00
11	1	4.10	18	1	10.63	10	1	6.22	15	1	10.36
13	1	9.19	19	1	7.20	18	1	7.79	16	1	8.06
14	1	7.73	21	1	9.75	22	1	8.79	21	1	8.44
19	1	10.31	22	1	7.87	24	1	9.84	23	1	6.92
23	1	10.92	23	1	6.48	25	1	13.16	25	1	12.51
25	1	14.01	24	1	8.99	29	1	11.51	27	1	11.68
27	1	13.17	26	1	11.44	30	1	13.92	29	1	13.92
29	1	9.68	28	1	13.55	32	1	10.66	30	1	13.22
30	1	8.36	33	1	14.78	33	2	12.26	31	1	9.35
35	1	12.05	35	1	12.25	34	1	12.45	34	2	12.70
36	2	12.78	36	2	12.91	37	2	10.85	35	2	11.22
38	2	8.63	37	2	11.94	38	2	8.57	37	2	9.64

40	2	11.86	38	2	9.39	43	2	5.52	39	1	14.75
41	2	9.86	40	2	13.76	44	2	10.22	40	1	15.60
42	2	7.33	42	2	7.06	47	2	14.32	49	2	11.82
45	2	11.33	45	2	10.09	48	2	13.50	50	2	10.44
46	2	10.55	46	2	14.56	49	2	12.84	52	2	6.11
53	2	5.90	47	2	11.12	50	2	9.39	54	2	4.75
55	2	4.89	55	2	5.47	51	2	11.38	58	2	3.25
58	2	3.36	58	2	3.91	53	2	7.13	61	2	5.44
61	2	6.52	60	2	4.69	60	2	4.61	62	2	7.50
62	2	8.05	64	2	8.59	62	2	6.38	64	2	8.98
64	2	9.31	65	2	7.90	63	2	7.88	65	2	8.34
65	2	4.16	66	2	6.27	68	2	3.56	67	2	6.83
69	2	1.96	68	2	3.05	69	2	2.80	69	2	3.91

Experiment 3-13			Experiment 3-14			Experiment 3-15			Experiment 3-16		
Position	Exit	Time	Position	Exit	Time	Position	Exit	Time	Position	Exit	Time
1	1	8.93	4	1	5.86	3	1	5.32	2	1	7.75
2	1	7.51	5	1	4.44	4	1	6.11	3	1	6.54
3	1	8.20	8	1	3.69	5	1	4.36	4	1	9.43
5	1	3.74	13	1	8.59	12	1	4.81	5	1	5.89
6	1	2.39	15	1	6.97	13	1	12.35	6	1	3.63
9	1	4.94	16	1	9.16	15	1	8.42	8	1	4.84
14	1	9.91	17	1	12.97	18	1	11.63	10	1	7.07
16	1	11.44	18	1	11.31	20	1	9.12	14	1	10.03
18	1	12.12	22	1	5.22	22	1	7.83	15	1	8.38
21	1	6.53	24	1	7.69	23	1	7.24	16	1	11.94
23	1	5.65	25	1	9.83	25	1	15.09	18	1	14.35
26	1	10.71	33	2	16.40	26	1	10.29	19	1	8.88
28	1	13.83	34	1	12.17	27	1	13.91	26	1	10.97
29	1	14.86	37	1	10.51	29	1	13.11	28	1	12.64
30	1	12.92	39	2	14.53	31	1	11.01	30	1	13.35
34	2	12.37	41	2	11.99	35	2	13.93	31	1	14.96
35	1	15.45	44	2	11.20	38	2	13.21	32	1	15.50
36	2	11.66	45	2	13.78	40	1	15.82	33	2	12.04
39	2	11.14	51	2	9.38	42	2	6.88	43	2	6.01
42	2	10.32	52	2	15.53	44	2	11.19	44	2	7.86
44	2	7.46	53	2	10.33	45	2	14.68	45	2	11.36
47	2	9.52	54	2	3.68	46	2	12.18	46	2	10.67
49	2	8.15	55	2	7.78	50	2	9.52	49	2	9.87
50	2	6.22	57	2	6.98	51	2	7.76	50	2	8.53
53	2	8.78	60	2	5.41	52	2	10.38	51	2	9.23
56	2	4.54	62	2	6.12	53	2	8.54	53	2	5.18
57	2	3.53	63	2	8.51	57	2	5.17	58	2	3.43
62	2	6.80	64	2	12.89	59	2	4.26	65	2	6.95
66	2	5.52	68	2	4.53	65	2	6.01	67	2	4.37

68	2	2.43	69	2	2.75	69	2	3.30	70	2	2.36